Transportation Geotechnics 46 (2024) 101256

Contents lists available at ScienceDirect

Transportation Geotechnics

journal homepage: www.elsevier.com/locate/trgeo

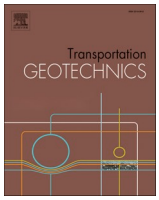

Original Article

Sustainable solutions for railway using recycled rubber

Yujie Qi *, Buddhima Indraratna, Trung Ngo, Chathuri M.K. Arachchige, Suwan Hettiyahandi

Transport Research Centre, School of Civil and Environmental Engineering, University of Technology Sydney, Ultimo, NSW2007, Australia

ARTICLE INFO

Keywords:
Recycled rubber
Railway tracks
Large-scale laboratory tests
Field tests
Sustainability

ABSTRACT

This paper introduces four innovative applications of waste rubber from scrapped tyres or conveyor belts in railway tracks. They include (a) a synthetic energy-absorbing layer of coalwash, steel furnace slag and rubber crumbs (SFS + CW + RC) for railway subballast, (b) a rubber inter-mixed ballast system (RIBS), (c) energy-absorbing rubber geogrids, and (d) a hybrid track incorporating tyre cells and elements of off-the-road truck tyres. Comprehensive laboratory and field tests have been conducted to investigate the geotechnical properties of these applications. Specifically, an empirical model was developed to predict the permanent deformation response of SFS + CW + RC mixtures that incorporate the effect of granular rubber and axial loads based on cyclic triaxial tests. Large-scale triaxial tests and field trials proved that RIBS exhibited improved energy-absorbing properties, sufficient shear strength and the promising ability to mitigate ballast breakage and stress distribution. A rubber geogrid with an optimal rib thickness of 10.6 mm was selected based on drop-hammer impact tests. The performance of the hybrid track was investigated using the National Testing Facility for High-speed Rail (NTFHR), from which it was found that the reinforced track had significantly less settlement, lateral deformation and ballast breakage than the traditional track.

Introduction

Railway networks play a crucial role in providing connectivity and accessibility, particularly across broader geographic areas such as Australia. Despite rail transport being generally more efficient and producing fewer emissions per passenger or ton-mile than car travel or truck transportation, the ever-increasing pressure from urban development necessitates faster and heavier rail networks. As a result, ballasted track deteriorates faster via ballast breakage, differential settlement, mud pumping, and track bulking, which leads to costly and frequent track maintenance. In the period of 2021–2022 alone, around $2.13 billion was spent on rail track maintenance in Australia[62], which is not only expensive, it also has an adverse impact on the landscape and the environment; moreover, the actual loss in productivity due to regular maintenance and track upgrading can be more than threefold. This means that railway industries are facing inevitable challenges given that high-quality natural aggregates are becoming increasingly scarce and environmental legislation is becoming more stringent. There is therefore, increasing pressure to explore innovative and more sustainable solutions for future railway construction.

To solve these challenges, researchers are endeavouring to introduce recycled and marginal materials (e.g. waste tyre products, mining by-products, demolition waste, recycled glass and plastics) into rail track foundations in order to minimise technical problems with rail track while remaining environmentally friendly and economically attractive [18,42,41,31,4,14,80,15]. Of these possible solutions, recycled rubber products are the most prevalent given their high damping and ductility properties [39,58,35,51,54,61,43,53].

It has been reported that recycled rubber mats/pads (under ballast mats and under sleeper pads) made from waste tyres or conveyor belts can increase the contact area at the ballast-subballast and ballast-sleeper interface and thus reduce the concentration of stress and ballast breakage [12,36,44,32,29]. When the sidewalls of recycled tyres are removed and the tyres are filled with recycled ballast, they can be used in the capping layer to enhance the confining pressure and increase track stiffness and thus reduce lateral dilation and ballast settlement [34]. Arachchige et al. [1–2] and Indraratna et al. [20] mixed recycled rubber granules with ballast and received promising laboratory and field trial results with reduced ballast degradation and settlement. Moreover, a synthetic energy-absorbing composite for railway subballast was developed by mixing recycled rubber crumbs (RC) and mining by-products including coalwash (CW) and/or steel furnace slag (SFS)

* Corresponding author.
E-mail addresses: yujie.qi@uts.edu.au (Y. Qi), Buddhima.indraratna@uts.edu.au (B. Indraratna), Trung.Ngo@uts.edu.au (T. Ngo), chathuri.arachchige@student.uts.edu.au (C.M.K. Arachchige), suwan.hettiyahandi@student.uts.edu.au (S. Hettiyahandi).

https://doi.org/10.1016/j.trgeo.2024.101256
Received 18 March 2024; Received in revised form 16 April 2024; Accepted 18 April 2024
Available online 21 April 2024

[28,52,47,19,30]. They found that an optimal SFS + CW + RC mixture would act like an energy-absorbing reservoir that would reduce ballast breakage and track vibration [47,49,52]. Moreover, the commercial use of SFS and CW as civil engineering fills above and under the groundwater level was approved by the New South Wales Environment Protection Authority [7]. The durability of recycled rubber is not a problem given that it is not exposed to UV or heat when buried underground, and its chemical leachability is low under normal conditions for civil engineering applications [13,16].

This paper will review four innovative applications of recycled rubber in railways: (1) a synthetic energy-absorbing layer of SFS + CW + RC for subballast, (2) Rubber intermixed ballast system (RIBS), (3) energy absorbing rubber geogrid, and (4) a hybrid track combining tyre cells with large off-the-road truck tyres. More specifically, the permanent deformation behaviour of SFS + CW + RC mixtures have been investigated using small-scale cyclic triaxial tests. The performance of rail tracks incorporating RIBS, rubber geogrid, and the hybrid track have been investigated using the large-scale triaxial apparatus, drop-hammer impact loading apparatus, prototype National Testing Facility for High-speed Rail (NTFHR), and field trials.

SFS + CW + RC Mixtures for Rail Subballast

The proposal to use a synthetic energy absorbing layer consisting of SFS, CW and RC mixtures was inspired by the successful use of SFS + CW mixtures for port reclamation [11]. The combination of SFS and CW would counteract the adverse characteristics of both materials, i.e., the volume instability of SFS and the particle breakage of CW. The introduction of rubber crumbs into SFS + CW mixtures will further suppress the adverse effect of SFS and CW and also improve the energy-absorbing property of the mixture; this will further reduce the particle degradation of ballast and load propagation to the under-laying subgrade. However, these recycled and marginal materials differ from traditional materials hence the general deformation mechanism of granular soil cannot directly apply to them. Therefore, it is imperative to investigate the deformation behaviour of SFS + CW + RC mixtures under cyclic loading, and also address the influence of rubber content and cyclic loads. To further facilitate this, an empirical model is also proposed to predict the permanent deformation response of waste mixtures with higher percentages of rubber under heavier loads.

Materials and Test Program

The source materials SFS and CW came from local mining industries in the Illawarra area of New South Wales, Australia, and the recycled rubber crumbs came from a waste tyre recycling company in Australia. The gradation curves of the waste materials and the mixtures are shown in Fig. 1. Note that the particle size distribution curves of the SFS + CW + RC mixtures align with the suggested gradation of the capping layer by Australian Rail Track Corporation[3]apart from a small discrepancy with the smaller particles which may compromise the hydraulic conductivity of the subballast layer. However, the falling-head permeability tests conducted by Indraratna et al. [28] indicated that the tested mixtures (rubber content ranging between 0 and 40 %) with ≥ 10% of rubber in mass satisfied the permeability requirement for subballast, i.e., the permeability coefficient $10^{-5} < k < 10^{-3} m/s$.

The cyclic triaxial test results from Qi et al. [50] were used in this paper to investigate the permanent deformation mechanism of the SFS + CW + RC mixtures with varying amounts of rubber (0, 10, 20, 30, and 40 %, by mass) and a fixed mixing ratio of SFS:CW = 7:3 (by mass). The cyclic loading tests (sample size: 50 mm in diameter, 100 mm in height) were conducted under confining pressures of $\sigma'_3 =$ 10, 40 and 70 kPa with a loading frequency of 5 Hz. These applied confining pressures covered the low to medium confinement range for railway subballast, and the loading frequency was low enough to eliminate the mass inertia effect of the test specimen [59]. The maximum deviator stress was determined by $q_{max,cyc} = 2\sigma'_3 \bullet CSR$, where CSR is the cyclic stress ratio. In the test a CSR = 0.8 was used, which resulted in $q_{max,cyc} =$ 16, 64, and 112 kPa. All the tests were completed by 50,000 cycles. Details of sample preparation and test procedures can be referred to Qi et al. [50].

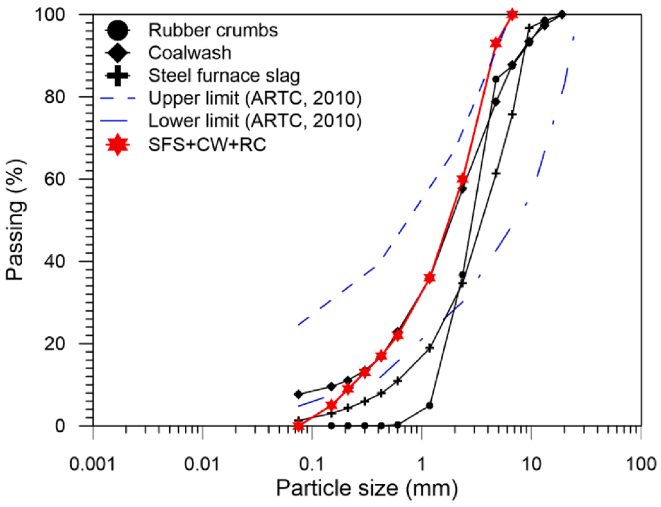

Fig. 1. Gradation of source waste materials and their mixtures.

Permanent Deformation

The permanent deformation behaviour of waste aggregates under cyclic loading can be classified into three categories based on materials' responses related to the permanent axial strain rate[9,46,55], as shown in Fig. 2: (1) Range A, plastic shakedown. After a certain number of loading cycles the axial strain of the test specimen stabilizes with an insignificant axial strain rate (i.e., $\dot{\varepsilon}_p < 10^{-8}$; this indicates that this material will achieve a long-term steady state under cyclic loading, which is preferable to be used as a railway subballast layer; (2) Range B, plastic creep. As indicated by Fig. 2, the axial strain of the test specimen ending with plastic creep will continue to increase to the end of the test (i.e., 50,000 cycles) with a faster axial strain rate $10^{-8} \le \dot{\varepsilon}_p < 10^{-7}$ than Range A; (3) Range C, incremental collapse. The typical phenomenon is that the axial strain rate of the test specimen decreases slowly or even increases ($\dot{\varepsilon}_p \ge 10^{-7}$ at 50, 000 cycles), this results in a fast accumulation of axial deformation and then the material fails.

The axial strain responses of SFS + CW + RC mixtures are shown in Fig. 3. It is noted that the axial strain increases as the amount of RC in the mixture and the deviatoric stress increase (Fig. 3a-c). Under a low deviator stress ($q_{max,cyc} = 16kPa$), all the mixtures stabilize quickly after 10 cycles and then reach plastic shakedown where the axial strain rate is between 10^{-9} and 10^{-8} (Fig. 3ad). When the deviator stress is higher (i.e., $q_{max,cyc} = 64 and 112kPa$) only those waste mixtures with 0 and 10 % of rubber achieve plastic shakedown, all the others end up with plastic creep (Range B) (Fig. 3bcef). These test results indicate that SFS + CW + RC mixtures with RC content ≥ 20% are not suitable for railway foundations because materials with a plastic creep response will eventually end up with a large settlement when the loading cycles are more than 50,000 cycles. Due to the stringent control of railway settlement (axial strain ≤ 2 %) in Australia[3], SFS + CW + RC with 10 % RC is preferable given its promising performance in deformation shown in Fig. 3, apart from reducing ballast breakage and track vibration, as reported by Qi et al.[47,52,52,47,49].

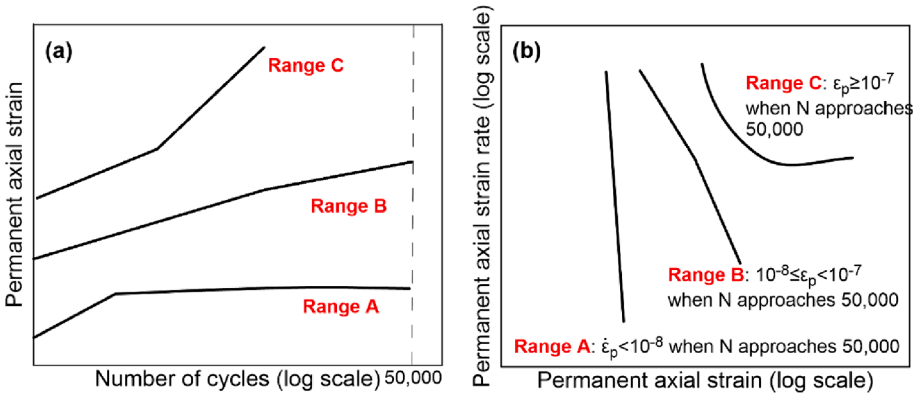

Fig. 2. Permanent deformation behaviour for waste granular materials (modified after [48].

Empirical Model

To further explore the influence of the amount of rubber and the deviator stress on the deformation response of SFS + CW + RC mixtures. An empirical model to predict the permanent axial strain rate $\dot{\varepsilon_p}$ was developed by Qi and Indraratna [48] to capture the effect of cyclic deviator stresses, the amount of rubber, and the number of loading cycles; the model is shown below:

$$\dot{\varepsilon_p} = \left[(A_1 q_{cyc,max} + A_2) \bullet \ln(R_b + 1) + (B_1 q_{cyc,max} + B_2)\right] \bullet N^{m \bullet R_b + n} \quad (1)$$

where A_1, A_2, B_1, B_2, m and n are the material constants with values of 3.69×10^{-5}, -2.40×10^{-4}, 5.40×10^{-5}, 0.004, 0.0042, and −1.448, respectively; R_b (%) is the amount of rubber. Based on this empirical model, the permanent deformation of waste mixtures with a higher amount of rubber under higher cyclic deviatoric stress can be predicted to 50,000 loading cycles, as shown in Fig. 4. It is noted that $q_{max,cyc} = 166kPa$ is equivalent to the axial stress under a freight train with a 30-ton axle load. The predicted results indicate that as the cyclic deviator stress and amount of rubber increase, the mixtures tend to have a higher permanent axial strain rate reaching 50,000 loading cycles, and the permanent deformation behaviour changes from plastic shakedown (Range A) to plastic creep (Range B) and then to collapse (Range C). It is noted that under heavy haul loading, when $R_b > 62$ %, the mixture will fail and the mixtures with $R_b < 15$ % will achieve plastic shakedown, as indicated by the prediction. Please note the proposed Equation (1) is limited to rubber crumbs, while rubber products with other shapes such as rubber shreds/chips and rubber fibre will be investigated in the future.

Rubber Intermixed Ballast System

Rubber Intermixed Ballast Stratum (RIBS) is a concept of using rubber granules from waste tyres as an engineered solution where natural rock aggregates (ballast) are appropriately blended with rubber granules to enhance the performance of ballasted rail tracks [1–2]. More significantly, substituting a fraction of the ballast weight with rubber particles possessing comparable angularity and measuring between 9.5 and 19 mm will mitigate the particle breakage of load-bearing larger rock particles and effectively reduce the risk of ballast fouling. The ultimate gradation of RIBS complies with the Australian standard for ballast material [5]. To investigate the geotechnical behaviour of RIBS and the performance of track incorporating RIBS, large-scale monotonic triaxial tests and field trial results were conducted.

Stress–strain Response

Monotonic loading triaxial tests (sample size 300 mm in diameter and 600 mm high) were carried out following ASTM-D7181 [6] guidelines and maintaining drained conditions. These experimental procedures were conducted with varying mass percentages of rubber ranging from 0 % to 15 % in the RIBS mixture, to evaluate the influence of rubber on the efficacy of the ballast and ascertain its conformity to anticipated standards. Each specimen underwent axial strains ranging from 20 % to 25 % until failure or until they reached the maximum axial deformation limit of the test facility. The loading rate was set at 1.5 mm/min to prevent the accumulation of excess pore pressure and to maintain drainage. This section examines the impact of the rubber content (R_b) under varied effective confining pressures ($\sigma_3^{'}$ = 30–60 kPa) on the stress–strain behaviour of RIBS and also compares the findings with conventional ballast material.

Fig. 5 shows typical stress–strain responses for RIBS mixtures with varying R_b percentages (0 %, 5 %, 10 %, and 15 %) at confining pressures of 30 and 60 kPa. The deviator stress (q) of all the samples increases with the axial strain (ε_a) until it reaches the peak deviator stress (q_{peak}). The peak deviator stress ratio (q_{peak}) is indicated by a solid dark circle on each plot (Fig. 5a). There was no significant strain-softening observed in the tested materials under confining pressures of 30 and 60 kPa. This observation matches the observation that the samples underwent bulging towards the centre rather than a distinct shear plane with the increased loading. It can be seen that the q_{peak} rises with the effective confining pressure but decreases with increasing R_b (>5%) under the same pressure. However, at$R_b = 5$ % the RIBS mixtures exhibit a similar q_{peak} to pure ballast, but with more rubber, the samples become rubber-like, shifting from brittle to ductile behaviour.

Unlike light tamping, increased deviator stresses and effective confining pressures compress the rubber particles, which results in a more compressive behaviour than the samples without rubber (Fig. 5b). Compressed rubber particles enhance effective particle interlocking and densify the granular matrix. RIBS samples with 5 % or no rubber exhibit minimal initial volumetric contraction, while RIBS mixtures with$R_b > 5$ % experience significant initial compression before dilation. Increased R_b in RIBS at larger confining pressures results in more substantial compression, potentially leading to initial settlement in the ballast layer. Abrupt fluctuations in the stress–strain curves indicate ballast breakage or particle surface attrition during shearing, diminishing with an increased amount of rubber. This suggests reduced ballast breakage due to enhanced contact surface area between the ballast and rubber, promoting interlock and resisting slipping, thus reducing stress concentrations at the particle contacts.

Peak Friction Angle

Experimental findings for RIBS indicate that the confining pressure and amount of rubber significantly influence the peak friction angle (φ_p). Here, the peak friction angle (φ_p) was calculated using the equation $\left(\frac{\sigma_1^{'}}{\sigma_3^{'}}\right)_p = \frac{1+\sin\varphi_p}{1-\sin\varphi_p}$, where φ_p represents the mobilized friction angle at the

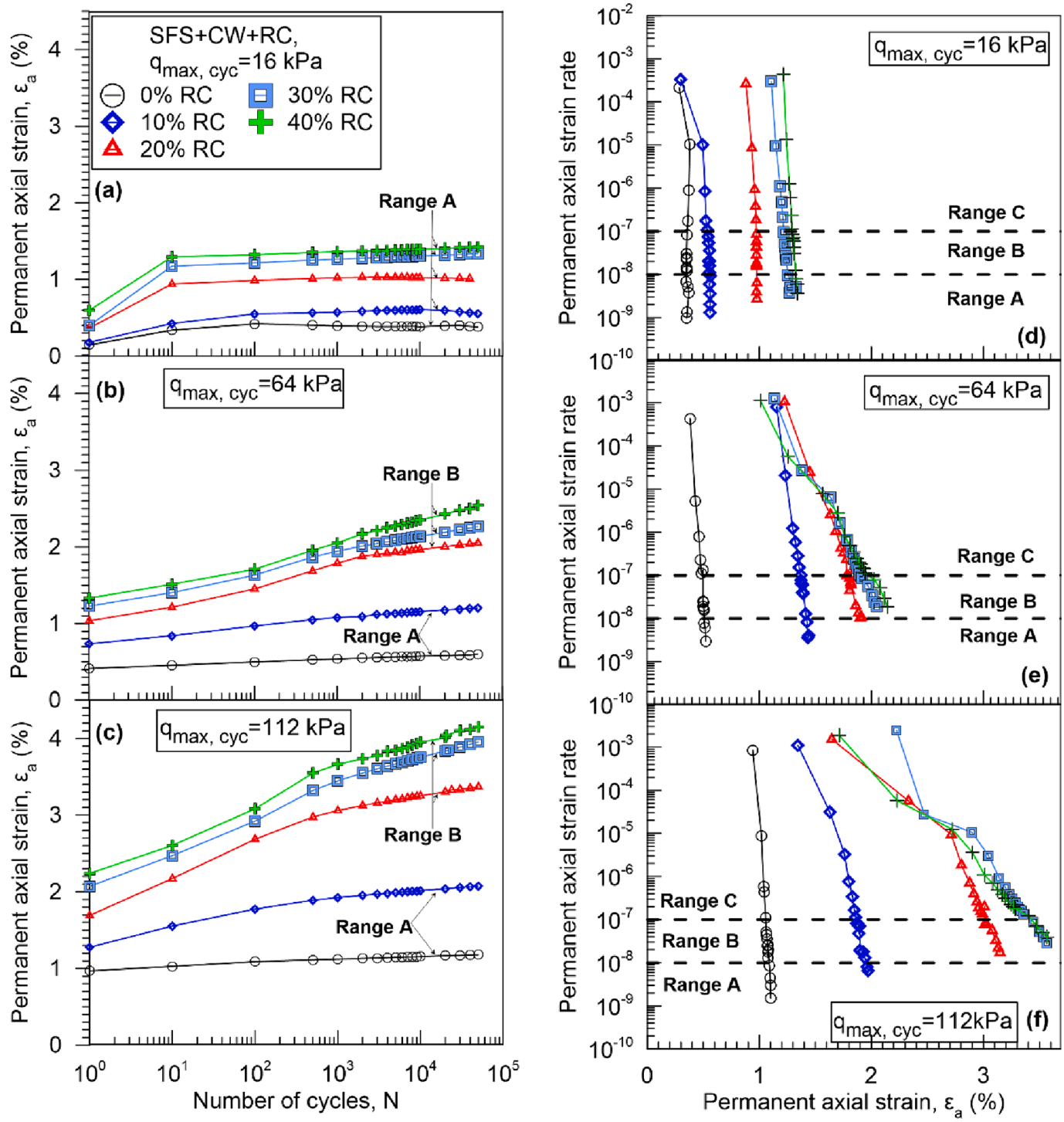

Fig. 3. Permanent axial strain and its changing rate for SFS + CW + RC mixtures (modified after [48].

peak stress ratio $\left(\frac{\sigma_1'}{\sigma_3'}\right)_p$. Fig. 6 shows the φ_p varying with the confining pressure of RIBS and also compares the test result from a previous investigation by Indraratna et al. [21]. It is noteworthy that the current study aligns with the literature whereby increasing the effective confining pressure decreases the peak friction angle of pure ballast and RIBS. Nevertheless, the peak friction angles of pure ballast obtained from Indraratna et al. [21] are greater than those in the current study due to the differences in particle gradation (i.e., varying coefficient of uniformity C_u) and the initial compaction status (i.e., varying void ratio e_0) of the samples. Moreover, the φ_p of pure ballast is similar to RIBS with 5 % rubber, but then it decreases with the amount of rubber ($R_b > 5$ %). This indicates that when $R_b > 5\%$, the shear strength of RIBS will be reduced as the amount of rubber to ballast and rubber to rubber contacts increase.

Energy Absorption

The capacity of the RIBS mixture to absorb energy is evaluated by employing the strain energy density (E_d)[17]:

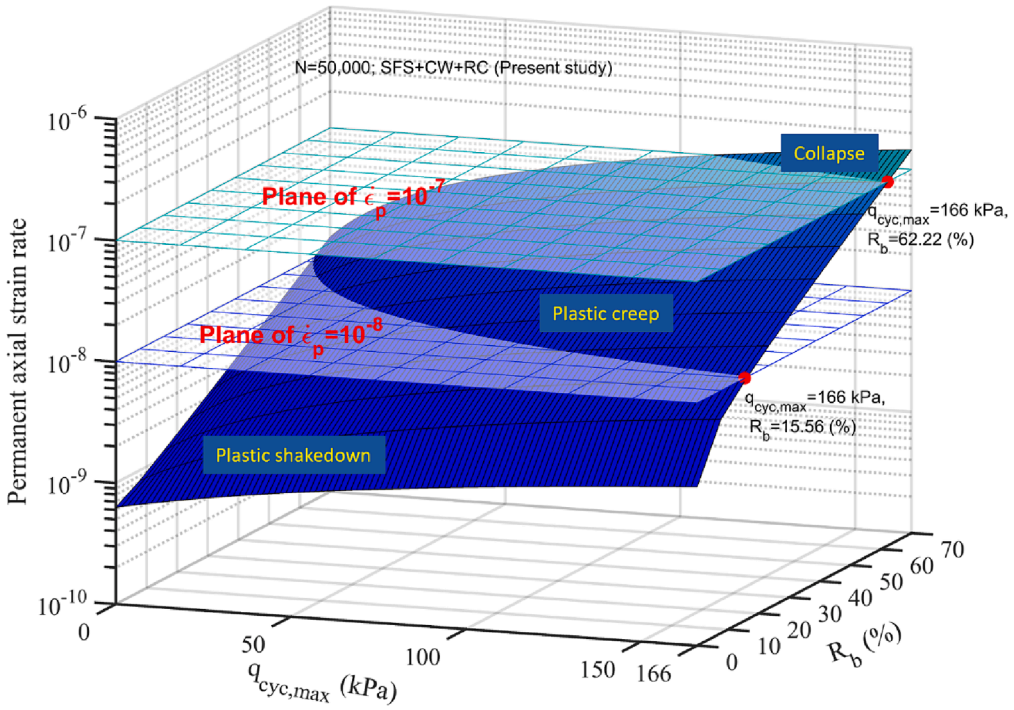

Fig. 4. Model prediction of the permanent strain response (modified after [48].

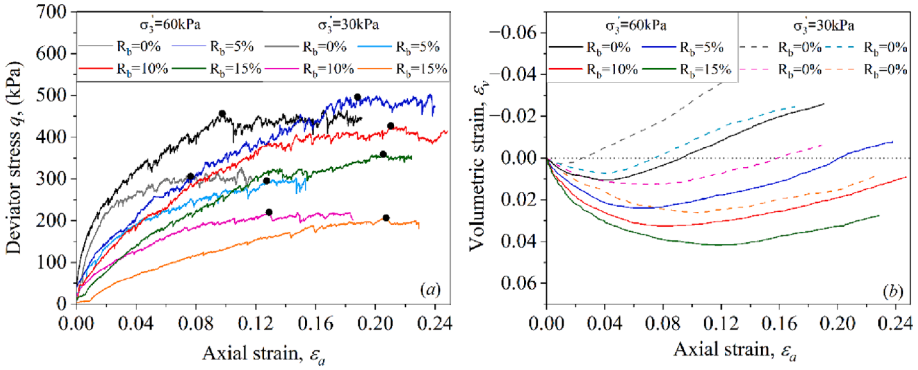

Fig. 5. Stress–strain response of RIBS (a) deviator stress-axial strain curves, (b) volumetric strain-axial strain curves (modified after [1].

$$E_d = \int_0^{\gamma_f} \tau d\gamma \tag{2}$$

where γ_f is the shear strain up to the peak shear stress and τ is the shear stress; here $\tau = q/2$, the shear strain is $\gamma = 3\varepsilon_q/2$ and ε_q is the deviator strain $\varepsilon_q = \varepsilon_a - \varepsilon_v/3$.

Fig. 7a shows the shear stress-shear strain curves of RIBS under an effective confining pressure of 30 kPa. The points where the shear stress stabilises are identified as the peak shear stress (γ_f) points. In Fig. 7a the shaded region under the shear stress–strain curve, up to the peak shear stress point, expands with the addition of more rubber due to the increased ductility, indicating an increase in strain energy density (E_d). The calculated E_d for RIBS material with varying R_b is shown in Fig. 7b. Note that the introduction of rubber amplifies E_d which suggests an increase in the energy absorption capacity of RIBS. The rationale behind incorporating rubber into ballast lies in the increased energy absorption capacity of the ballast layer. This not only mitigates internal ballast degradation but also minimises the transfer of energy to other underlying layers such as the subballast/capping layer and subgrade; this minimizes the deterioration of the overall track elements. As reported by Arachchige et al. [1], the ballast breakage of RIBS with 5 % or more of rubber was 50–60 % less than the pure ballast.

Distortional Energy

The strain energy density as proved in the previous section increases as rubber content in RIBS increases, and it consists of two components: distortional energy and volumetric energy. The distortional energy contributes to particle friction and breakage and the volumetric energy contributes to the deformation of the mixture [47,52]. Fig. 8a shows the change in the deviatoric stress ratio ($\eta = q/p'$) with respect to the deviator strain (ε_q) for RIBS with 0 and 5 % rubber, as represented by curve-1 and curve-2, respectively. The shaded area between curve-1 and curve-2 refers to the incremental distortional energy (ΔU) when R_b is reduced from 5 % to 0 %; it can be expressed as shown in the equation below

$$\Delta U = \int_0^{\infty} (\eta_2 - \eta_1) d\varepsilon_q \tag{3}$$

If $\Delta \rightarrow 0$, The differential incremental distortional energy will be,

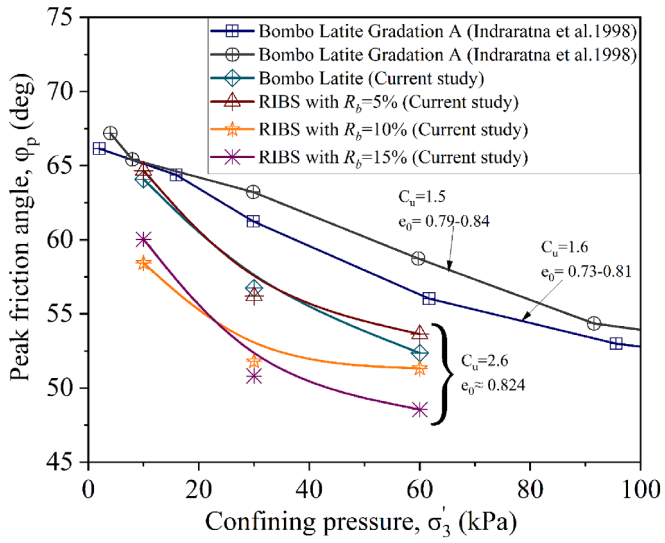

Fig. 6. Peak friction angle of RIBS.

$$du = \eta_2 d\varepsilon_q - \eta_1 d\varepsilon_q \tag{4}$$

$$\Delta U = \int_{\varepsilon_q=0}^{\varepsilon_q=\varepsilon_q^*} du = \int_{\varepsilon_q=0}^{\varepsilon_q=\varepsilon_q^*} \eta_2 d\varepsilon_q - \int_{\varepsilon_q=0}^{\varepsilon_q=\varepsilon_q^*} \eta_1 d\varepsilon_q \tag{5}$$

The distortional energy (U) at a given deviator strain (ε_q^*) can be determined using Equation (4) for RIBS with different R_b. Fig. 8b shows the distortional energy against the deviator strain for RIBS materials with varying rubber contents from 0 to 15 %, and the shaded area is the difference in the distortional energy ΔU due to adding rubber. All the plots can be empirically correlated with the deviator strain through a power relationship, i.e., Equation (6), where α' and β' are in a linear relationship with R_b% as shown in Fig. 8b.

$$U = \alpha' (\varepsilon_q)^{\beta'} \tag{6}$$

In Fig. 8a, the variation in energy computed between Curve 1 and Curve 2 signifies that the distortional energy absorbed by the mixture has decreased, whereas Fig. 8b shows that the curves rotate clockwise as R_b% increases. This indicates that as R_b increases, the distortional energy decreases, which then reduces the energy used for particle sliding and breakage. Furthermore, the reduced distortional energy indicates an increase in volumetric energy as the total strain energy increases (Fig. 7), which is why RIBS mixtures become more contractive but with less particle breakage when more rubber is added.

Field Trial

The Chullora rail precinct in Sydney was the site used for the field study where laboratory-validated RIBS technology was applied to actual railway tracks. This location encompasses industrial rail sidings utilized by Sydney Trains, the Australian Rail Track Corporation (ARTC), and Pacific National for loading, unloading, and maintenance activities. For experimental purposes, two 20 m-long sections of track were constructed as follows: (a) the RIBS section where RIBS material was placed in the ballast layer, and (b) the control section which only used conventional ballast material. The dimensions of the track design were determined by referencing the ARTC code of practice (Section 4 - Ballast), with typical ballast and capping thicknesses of 250 mm and 200 mm, respectively. A large-scale calibrated volumetric mixer was utilized to blend fresh ballast and rubber particles to the desired mix ratio (10 % rubber granules), while adhering to the particle size distribution outlined in the TfNSW ballast specifications [5]. In the RIBS

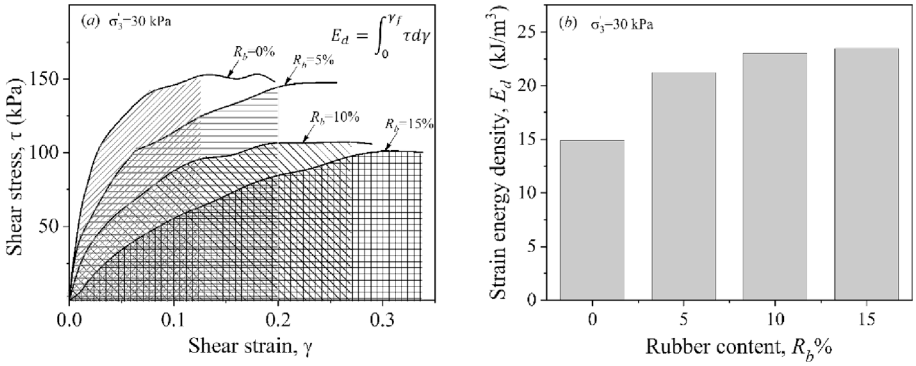

Fig. 7. (a) Shear stress-shear strain curves of RIBS, and (b) strain energy density varying with rubber contents.

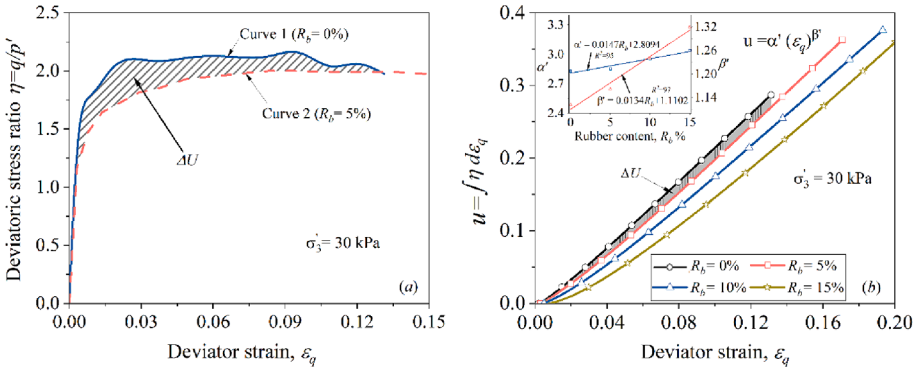

Fig. 8. (a) Incremental distortional energy (ΔU) (b) distortional energy (U) for RIBS with changing rubber contents.

section, approximately 150 mm of RIBS was used to replace the conventional bottom ballast layer, with the remaining ballast layer thickness achieved by adding a 100 mm layer of fresh ballast on top of the RIBS layer.

To assess track performance, a locomotive with a 21.5-ton axle load operated within the test sections at an average speed of 12 km/h to comply with the site speed limits. The locomotive was 21.15 m long and had two axles with a set of three wheels connected to each end. Pressure cells were placed at the interface of every substructure layer in the trial sections to measure the stress distribution across the depth, and an accelerometer was affixed to sleepers within each section to monitor track acceleration during locomotive operation. Fig. 9 shows the layout of the pressure cells at the interface between the ballast and capping layers and the placement of geotextile on top of the capping layer to prevent fine particles from infiltrating into the ballast layer.

Fig. 10 (a-c) shows the vertical pressure exerted at different interfaces within standard and RIBS track sections, including the sleeper-ballast, ballast-capping, and capping-subgrade interfaces. The plots show three peaks representing the vertical pressure generated by three wheels connected to one end of a single axle. Comparatively, the stress distribution within the RIBS track is lower than the standard track, especially at the ballast-capping interface where there is more than 30 % reduction in stress. There is also a 20 % reduction in vertical pressure at the ballast sleeper interface in the RIBS track which contributes to the reduction in ballast particle breakage in the top ballast layer.

Fig. 10d shows the vertical acceleration experienced by sleepers during locomotive operation. Peak acceleration on the standard track is approximately 0.06 g and around 0.2 g on the RIBS track, with 'g' representing acceleration due to gravity. This signifies a more than 60 % reduction in vertical acceleration on the RIBS track compared to the standard track. Furthermore, the RIBS track demonstrates minimal variation in acceleration during train operations, contributing to enhanced safety and improved passenger comfort by minimising track vibrations.

Energy Absorbing Rubber Geogrid

Polymer geogrids and resilient rubber components are commonly used to stabilize ballasted tracks. However, while traditional polymer geogrids help to minimise lateral deformation and vertical settlement they are prone to rupture under significant stress and cannot absorb energy. On the other hand, resilient rubber elements such as under ballast mats help to absorb energy but they impede the free drainage of water and do not reinforce the ballast. In this section energy-absorbing Rubber Geogrid is introduced, and this is a novel solution which merges the advantages of geogrids and resilient rubber components.

The rubber grids were manufactured from end-of-life rubber conveyor belts from the mining industry (Fig. 11a). These conveyor belts make up a significant portion of rubber waste[45]) and therefore reusing them as rubber grids is appealing from an engineering and sustainability perspective. Rubber grids secure ballast particles the same as traditional geogrids but also enable energy dissipation and shock absorption which reduces the impact on ballast[56]. This innovative approach improves track durability against vertical and horizontal stress, mitigates energy under repeated impact loads, lessens ballast wear and shape distortion, ensures proper drainage, and addresses the limitations of traditional geogrids and under ballast mats. In this section drop hammer tests were carried out to investigate the performance of ballast reinforced with rubber geogrid under impact load; the results, including the impact force, ballast deformation and breakage were then evaluated.

Large-scale Impact Loading Tests

Materials Used in the Study

In this study volcanic basalt aggregates sourced from quarries south of Sydney were used. They were meticulously washed, dried prior to being sieved and then mixed to the required gradation as per the Australian standards [5]. The apertures on the recycled rubber conveyor belt panels were cut with high-precision waterjet cutting (Fig. 11a-c). The engineering and mechanical properties of the rubber grid material are listed in Table 1. In this research three distinct types of rubber grid,

Fig. 9. Arranging pressure cells at the ballast-capping interface.

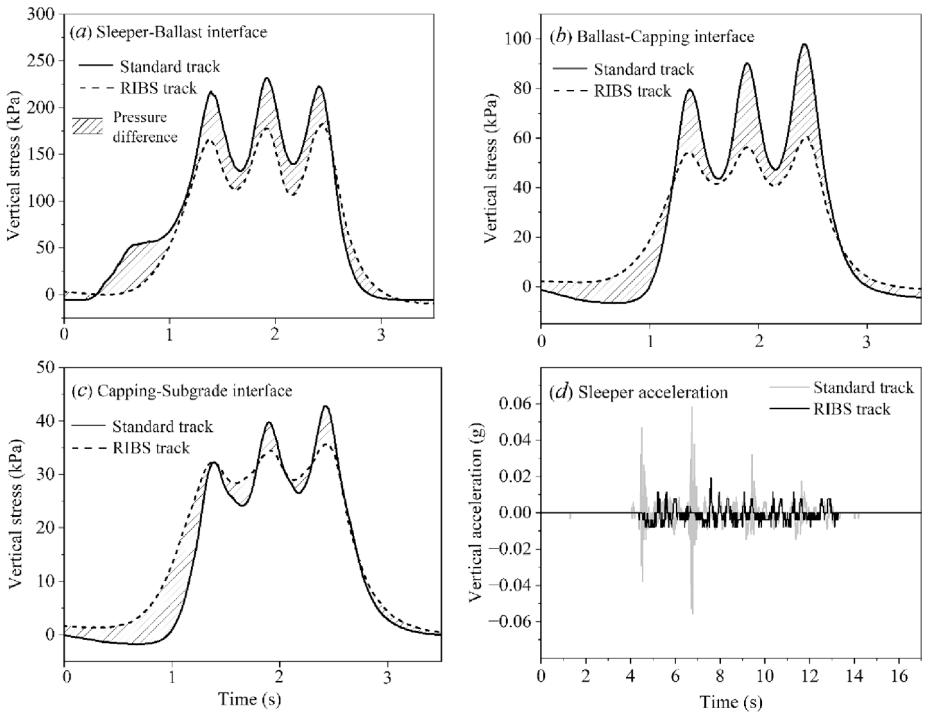

Fig. 10. Vertical pressure at (a) the sleeper-ballast interface (b) the ballast-capping interface (c) the capping-subgrade interface; (d) vertical acceleration of the sleeper.

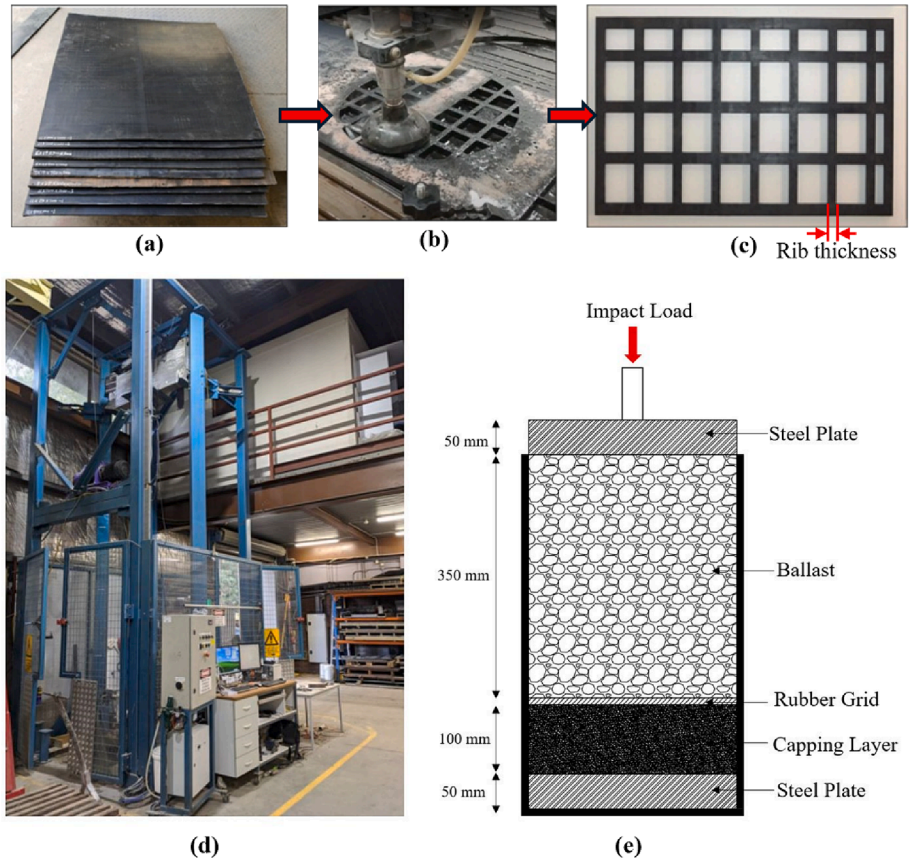

Fig. 11. (a) Recycled conveyor rubber panels, (b) waterjet cutting to make rubber geogrid, (c) rubber geogrid, (d) large-scale impact loading test apparatus, (e) schematic diagram of the test specimen (modified after [56].

Table 1
Engineering and Mechanical Properties of the Rubber Grid Material.

Parameters	Values
Thickness	10–11 mm
Aperture size	51 × 51*mm*
S1 Rib thickness	7.4 mm
S2 Rib thickness	10.6 mm
S3 Rib thickness	14.8 mm
Density	1.1 g/cm^3
Compressive strength at 2 % strain	100 kPa
Compressive strength at 5 % strain	750 kPa
Tensile Strength at 2 % strain	80 kPa
Tensile Strength at 5 % strain	180 kPa
Abrasion Resistance	81 mm^3
Hardness	60
Modulus of Elasticity	4 MPa

S1, S2, and S3, were utilized. Although all three types shared identical aperture shapes (square) and sizes of 51 × 51 mm, they differed in the thickness of their ribs, i.e. 7.4 mm, 10.6 mm, and 14.8 mm thick for S1, S2, and S3, respectively. The overall thickness of the grids was maintained between 10 and 11 mm.

Large-scale impact loading test apparatus and sample preparation

The impact test was carried out using a 5.81kN hammer falling from heights up to 6 m and reaching velocities up to 10 m/s. This system had a load cell on the hammer that was connected to a computerized data acquisition system to record the impact load. The hammer was lifted mechanically to a predetermined height and released onto the specimen by an electronic control. This setup, including the impact testing equipment and a diagram of a standard ballast sample prepared for lab tests, is shown in Fig. 11(d-e).

The ballast specimen (Fig. 11e), measuring 300 mm in diameter by 500 mm high, was encased in a 7 mm thick cylindrical rubber membrane. From bottom to top it included a 50 mm thick steel base plate, a 100 mm thick layer of sand and gravel (capping layer) compacted to 20.5 kN/m^3, a layer of rubber grid, and a 350 mm thick layer of ballast arranged in three compacted sub-layers to a bulk unit weight of 15.3 kN/m^3. This mimicked the initial density of Australian railway tracks and avoided any over-compaction and breakage. This setup was supported by a rigid steel mould to maintain a consistent diameter during sample preparation.

During the impact loading test the hammer was dropped 12 times per test from a height of 150 mm to simulate the typical dynamic impact stresses to which Australian railway tracks are subjected, especially in areas with rail corrugations, wheel wear, and transition zones [25]. The height and circumference of the specimen were measured at different points after the impact tests to assess any vertical and lateral deformation, after which the ballast was sieved and weighed to evaluate breakage. Four impact loading tests with and without rubber grids carried out by Siddiqui et al. [56] and one impact test for ballast reinforced with traditional polymer geogrid carried out by [25]were concluded in this section for better comparison.

Impact Forces

Under impact loading, two specific force responses were noted: initially, sharp force peaks (P_1) followed by smaller, more prolonged forces (P_2) within the first 300 milli-seconds of each drop. The initial sharp peaks (P_1) resulted from the inertia of the top-loading plate resisting the hammer's motion, with forces ranging between 345 and 410 kN, whereas the P_2 forces were significantly lower in magnitude and stabilized between 50 and 75 kN over a longer period. The effectiveness of rubber grids to reduce the impact forces is shown in Fig. 12, which also outlines changes in the P_1 and P_2 forces.

Typically, the P_1 and P_2 forces increase with each drop as the ballast assembly become denser, except for random variations of P_1 forces in the polymer geogrid-reinforced ballast. The rubber grid S2 shows the largest reduction in impact forces (P_1 decreases to 292 kN and P_2 decreases to 68 kN at drop N = 12), compared to the unreinforced ballast which has maximum forces of 387 kN (P_1) and 83 kN (P_2) measured at drop N = 12. The S1 rubber grid offers a slight decrease in these forces. The benefit of using rubber grid S3 to reduce the impact forces P_1 and P_2 is similar (slightly less) to rubber grid S2. However, using a conventional polymer geogrid does not lower the impact forces, rather, it increases the maximum P_1 force to 427 kN and P_2 to 87 kN measured at drop N = 12.

Deformation of Ballast

Fig. 13(a) and (b) display the axial (ε_a) and radial strains (ε_r), respectively. The radial strain was determined by averaging the circumferential strains recorded at three heights on the sample (bottom, middle, and top). As the number of drops (N) increases there is a

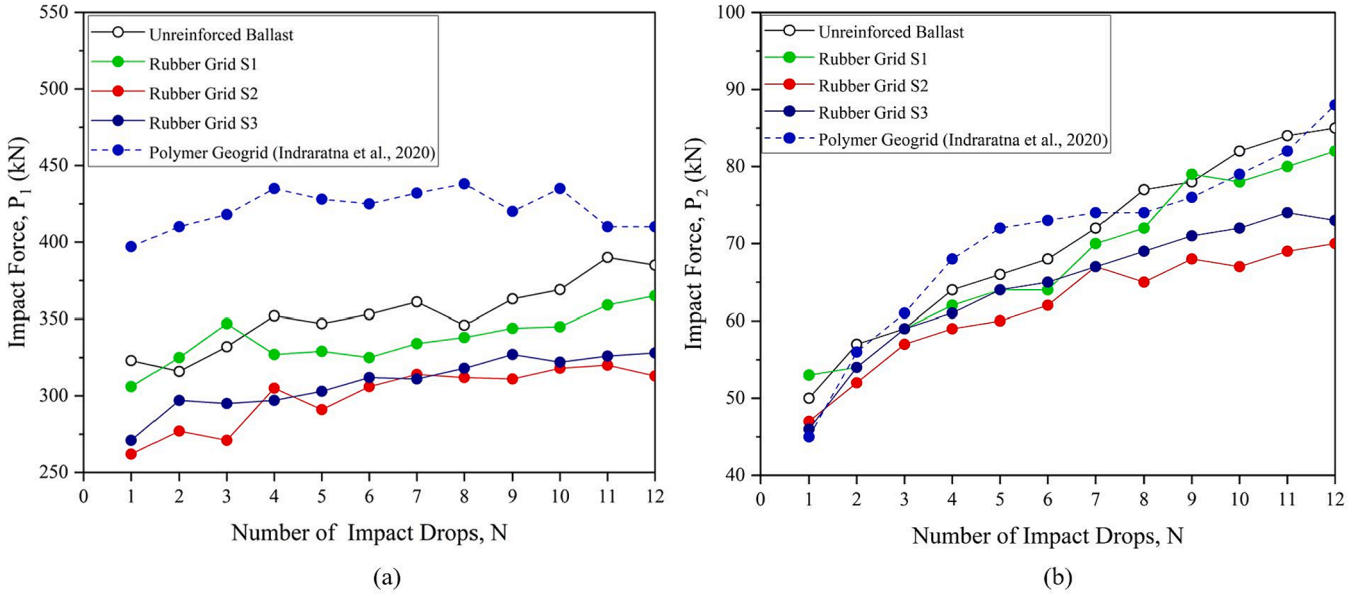

Fig. 12. The change of (a) P_1 and (b) P_2 with the number of applied impact loads (modified from [56].

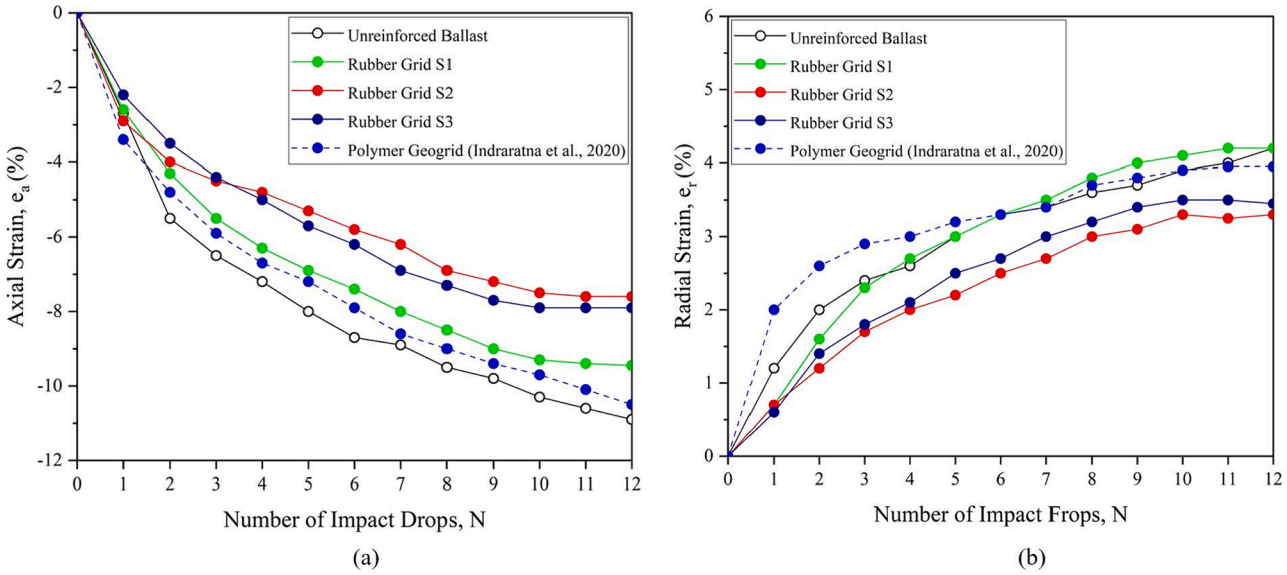

Fig. 13. The change of (a) Axial Strain and (b) Radial strain with the number of applied impact loads (modified from [56].

consistent rise in the axial and radial strains due to the vertical compression and lateral displacement of ballast aggregates. Overall, incorporating rubber grids reduces the axial and radial strains compared to tests with unreinforced ballast and those with traditional polymer geogrid. Moreover, with rubber grids, the axial and radial stains in the ballast gradually stabilise after the ninth drop, whereas the deformations of the test specimens with traditional geogrids and those without reinforcement keep on increasing.

Compared to the unreinforced specimen, rubber grid S2 effectively reduces the axial strain by up to 31 % and radial strain by 21 %, while rubber grids S3 and S1 reduced the axial strain by 29 % and 14 %, respectively; the S1 grid shows a negligible impact on radial strain. The inclusion of polymer geogrid reduces deformation slightly, with only 4.5 % and 5.7 % decreases in axial and radial strains, respectively.

Ballast Breakage

The ballast breakage index (BBI) introduced by Indraratna et al. [22] was used to quantify the breakage of ballast in this study (Fig. 14a). Fig. 14(b) presents the BBI measurements from various tests and highlights the ability of rubber grids to reduce ballast degradation. Specifically, the BBI for tests without reinforcement stands at 0.215, whereas the inclusion of rubber grids S1, S2, and S3 results in BBIs of 0.172, 0.141, and 0.135, respectively, thus showing how effectively rubber geogrids mitigate breakage. Notably, the S2 and S3 grids are the most effective because they reduce ballast breakage by up to 31 % and 33 %, respectively, whereas the S1 and the conventional geogrids exhibit 15 % and 30 % reductions in breakage, respectively. These findings reveal how effectively rubber grids reduce ballast degradation due to their ability to dampen impact forces and thereby reduce wear and decrease the energy transmitted to the ballast layer.

A Hybrid Track Incorporating Tyre Cell Reinforcement and OTR Segments

Ballast degradation is one of the major factors that seriously impair railway safety and efficiency, and thus necessitate reduced speed and increased track maintenance. Prior research has highlighted the

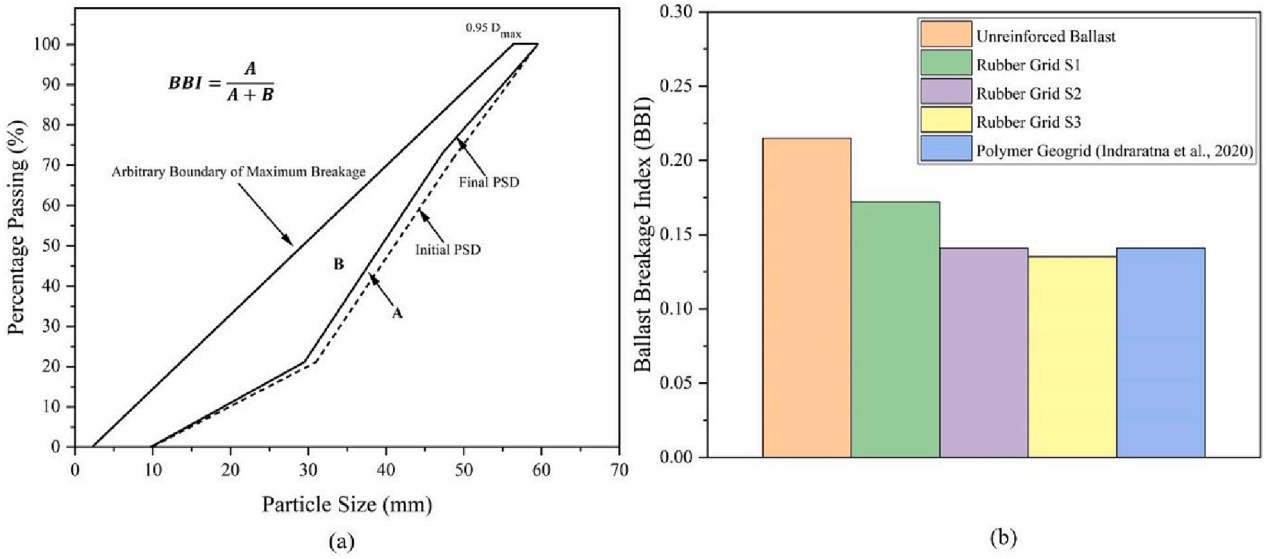

Fig. 14. (a) BBI calculation (b) Variation of BBI with different ballast reinforcements (modified from [56].

influence of confining pressure in track [37,60], confirming that the in-situ confining pressure is crucial in minimizing ballast breakage. On this basis, recent efforts have been made to prevent ballast breakage and improve the longevity of tracks with polymeric inclusions such as geogrids[8,10]to limit the lateral movement of particles and increase their confinement using geocells[40]. Waste rubber tyres have also been investigated in recent years to provide additional confinement for rail tracks. Indraratna et al. [34] performed tests on a single infilled tyre and found there was a substantial increase in the bearing capacity of the entire granular mass when an infilled tyre was present beneath the ballast layer. It is noted that waste tyres are sometimes burned for disposal convenience in some nations but this results in severe environmental damage and it could be the means of transmitting disease transmission in mosquito breeding seasons [57,45]. In addition, large off-the-road (OTR) tyres approximately 3 m in diameter and weighing over 3 tonnes are difficult to transport and to process them into crumbs.

This section proposes a novel approach by combining two concepts: (i) positioning an infilled tyre assembly beneath the lower ballast, and (ii) incorporating segments of OTR tyres into the shoulder ballast to increase the stability of the track substructure.

Role of Confining Pressure on Railway Track

While the impact of confining pressure on diverse geotechnical structures is crucial and is regarded as a vital criterion in their design, it is frequently undervalued in traditional rail track design and

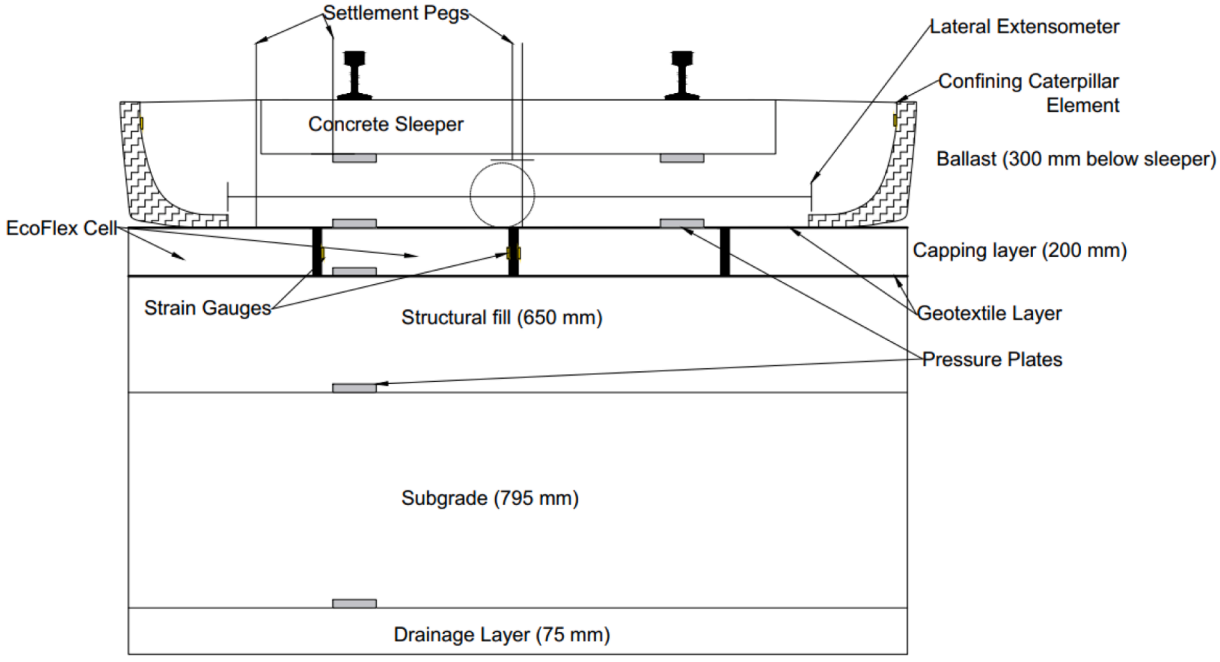

(a)

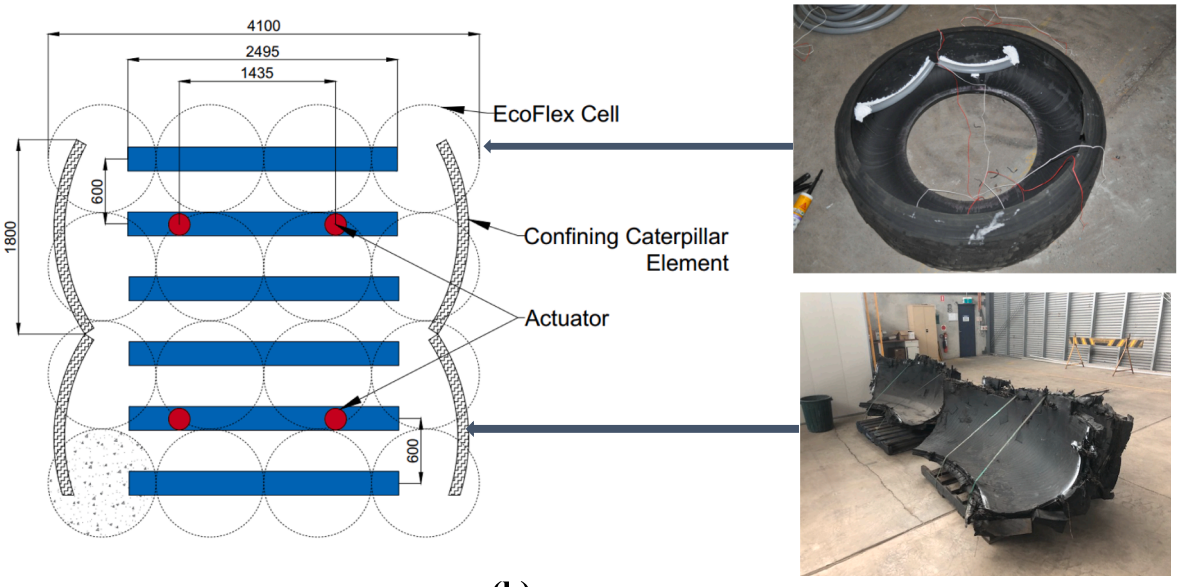

(b)

Fig. 15. (a) Cross-section of the hybrid track; and (b) schematic plane view of the track with Ecoflex tyre cells and shoulder-confined tyre segments.

construction. To ensure sufficient lateral stability, ballast can be extended beyond the sleepers, as suggested by Le Pen et al. [38]. Despite the intention of providing increased lateral stability through additional shoulder ballast, the in-situ confinement at track shoulders remains relatively low and this low pressure proves insufficient to control the excessive spreading of ballast. Indraratna et al. [33] concluded that the dilation and friction angle of ballast are influenced by the confining pressure, and optimized track confinement can lead to significant savings in track maintenance. Confinement in tracks is often very low (<30 kPa), which leads to significant dilation and breakage of highly angular ballast aggregates under cyclic loading. In this context, this section aims to use recycled rubber elements to increase the confinement for capping and shoulder ballast.

Test Program

The National Testing Facility for High-speed Rail (NTFHR), which the second author conceptually designed, can accommodate a variety of track conditions. This is the first facility of its kind in Australia. The NTFHR allows for conducting process simulation testing of tracks built over varied ground conditions to optimise their design and minimise construction and maintenance costs while enhancing track longevity. This facility can estimate the performance of recycled rubber inclusions, which could be scaled down for conventional (small-scale) laboratory equipment, but which would not provide a realistic output to convince the railway industry. Additional comprehensive information regarding the design, and construction for testing is available in Indraratna et al. [26]. In the first benchmark test, an unreinforced standard track was subjected to a 25-tonne load where f = 15 Hz (frequency) and run for 500,000 load cycles. In this study the NTFHR facility was utilised to examine the performance of the hybrid track where recycled rubber tyre cells (Ecoflex tyre cell) were assembled and infilled with spent ballast to replace the standard capping layer (subballast), and segments of OTR tyres were used to provide confinement. A cross-section of the hybrid track is illustrated in Fig. 15a and a schematic plane view of the track with Ecoflex tyre cells and shoulder-confined tyre segments is shown in Fig. 15b.

A total of 16 truck tyre cells, each with a diameter of 1 m and heights ranging from 275 to 300 mm were constructed (Fig. 16a). This arrangement of filled tyre cells will provide substantial lateral confinement, enhancing track stiffness, and will possess properties for absorbing energy to mitigate unnecessary vibration and noise. The tyre assembly was then covered with 300 mm thick layer of clean ballast to conform to Australian Standards[5]. The ballast was then compacted to achieve a unit weight of approximately 15.5—16.0 kN/m^3, as expected in Australian heavy haul tracks.

Giant OTR tyres with a radius of approximately 1700 mm and a tread width of around 1160 mm were used to confine the shoulder ballast (Fig. 16b). To accommodate the standard ballast layer height of 550 mm for a heavy-haul railway track, the tyre was cut into "L" shaped segments to reduce the length of the sidewall to 300 mm (Fig. 16c). These segments were strategically placed alongside the shoulder ballast to provide additional support. The resulting catenary was comparable in height to the standard layer of ballast and acted as a stabilizing force against lateral push in addition to its self-weight.

This experiment involved subjecting the system to cyclic loading conditions where F_{min} = 15 kN, F_{max} = 125 kN and F_{mean} = 70 kN, mimicking a 25-tonne axle load freight train. A frequency of f = 15 Hz was used to simulate typical heavy haul trains operating on Australian tracks and for comparison with the unreinforced test. The test took place

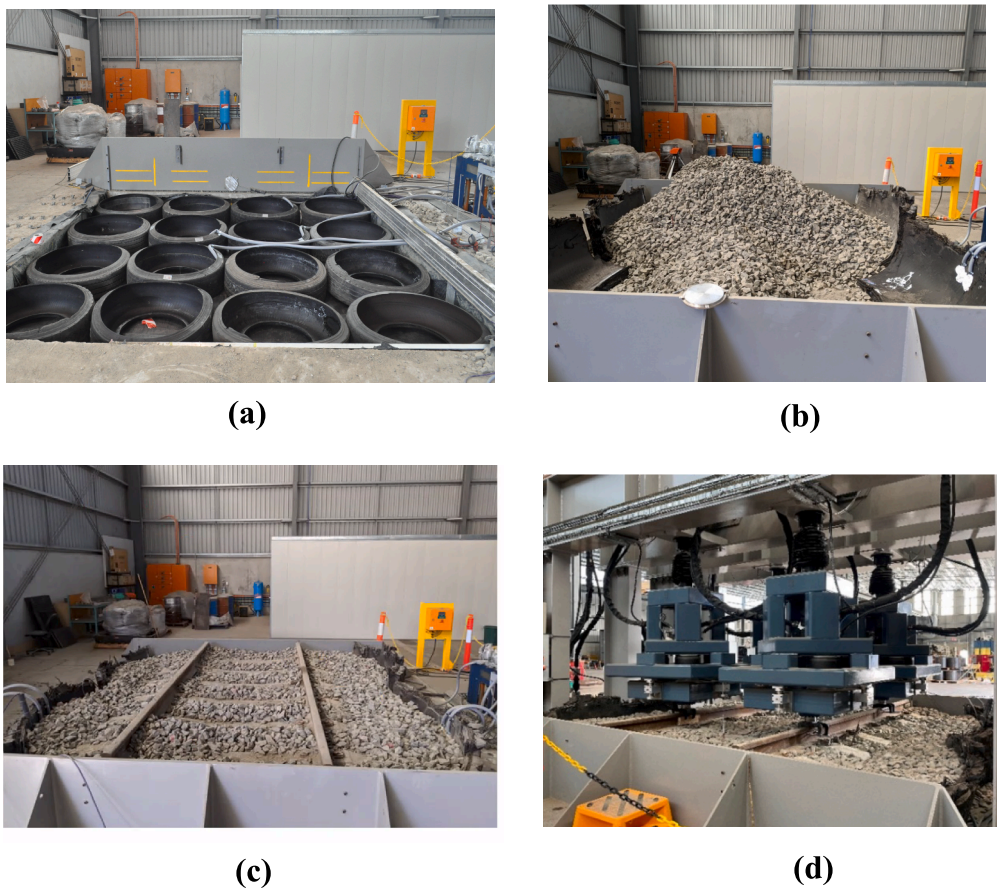

Fig. 16. (a) Recycled tyre assembly in capping; (b) Placement of tyre segments in ballast shoulder; (c) Finished track before testing; (d)Applied cyclic loading during the test.

with up to 500,000 loading cycles, during which lateral displacement, settlement, stress, and acceleration were monitored using an automated data acquisition system (Fig. 16d). The ballast was also sieved after the test to calculate the ballast breakage index (BBI). While comprehensive test set-ups and results have been presented by[23], selected test results were reported and compared with unreinforced standard track and field data obtained from Bulli and Singleton in New South Wales, as presented in the following sections.

Track Deformation

Fig. 17a compares the vertical settlement measured from the hybrid track with those discussed earlier for the standard test (unreinforced) using NTFHR (Indraratna et al. 2021); it also shows the results of laboratory tests using the large-scale track process simulation apparatus [24]and field measurements at Bulli, New South Wales, Australia [27]. Note that the initial sharp settlement (N = 100,000 cycles) occurs for all tests, followed by a gradual increase in displacement over the next N = 300,000 cycles, and then a stable settlement until the end. Interestingly, even though the hybrid track settles at a higher initial rate than the conventional (unreinforced) track tested by NTFHR and field trial due to the higher initial compressibility of the infilled rubber tyres, the overall accumulated settlement of the hybrid track is lower after 300,000 cycles. The settlement of the unreinforced track by NTFHR is almost identical to the field measurement, while the settlement of the hybrid track shares a similar but slightly higher pattern than the laboratory measurement. The hybrid track stabilises at around N = 100,000 which is much faster than the unreinforced track tested by NTFHR and in the field.

A comparison between the lateral displacement in the ballast layer measured in laboratory, the field, and NTFHR is shown in Fig. 17b. Note that the lateral displacement for NTFHR testing was recorded by two extensometers placed at different locations, with each measuring the total lateral displacement; this is denoted as Hybrid-1&2 and Conventional-1&2 in Fig. 17b. Here the lateral displacement (dilation) of every test increases rapidly at the initial loading stage and then gradually stabilizes. The unreinforced conventional track exhibits a notably higher average lateral displacement of approximately 8–9 mm by NTFHR, 11 mm by field test, and 8 mm by the laboratory test, whereas the hybrid track has an average lateral displacement ranging from 3 to 6 mm, with an overall average displacement of 4 mm. Without doubt the rubber catenary shoulder confinement effectively restricts the lateral spreading of ballast, because the inclusion of rubber elements provided more than double the confining pressure for the track (σ_n = 55 kPa), compared to σ_n = 23 kPa for the standard track [26].

Ballast Breakage

Once the hybrid test was completed, the ballast underneath the actuator and shoulder was recovered separately and passed through standard sieves to calculate the ballast breakage. Visual observations when collecting ballast after the test showed that ballast aggregates experienced various forms of degradation such as attrition, corner breakage, and abrasion. The degree to which recycled rubber elements mitigated ballast breakage can be examined using BBI to quantify and compare the shift in particle size distribution towards smaller particles caused by particle degradation, as previously shown in Fig. 14 and defined in Section 4. The reduction in the ballast breakage index R_{BBI} (%) due to the effects of recycled rubber elements is then determined as:

$$R_{BBI}(\%) = \frac{BBI_{Hybrid\_Track} - BBI_{Conventional\_Track}}{BBI_{Conventional\_Track}} \quad (7)$$

Compared to the BBI determined from the standard track [26], the application of rubber elements significantly reduces ballast breakage such that ballast collected from the hybrid trach from underneath the sleeper and shoulder has BBI = 0.087 and 0.043, compared to the conventional track with *BBI* = 0.143 and 0.075. As a result, the reduction in breakage for the hybrid track is R_{BBI} = 39.2 % for ballast collected underneath an actuator and an R_{BBI} = 42.7 % for shoulder ballast. As the overall track confinement is increased due to the catenary boundaries, ballast particles are effectively bound together with ample lateral confinement, thus ensuring an optimal internal contact stress distribution and inter-particle contact areas. Consequently, the potential for breakage due to the concentration of stress is mitigated.

Conclusions

This paper investigated four innovative applications of recycled rubber, they included mixing recycled rubber crumbs with CW and SFS for an alternative subballast layer, a rubber inter-mixed ballast system, rubber geogrid, and a hybrid track incorporating tyre cells in capping layer and truck tyre elements reinforcing the shoulder ballast. Comprehensive laboratory testing employing small and large-scale triaxial apparatus, large-scale drop-hammer impact loading facility and National Testing Facility for High-speed Rail (NTFHR) have been carried out to investigate the performance of these novel applications.

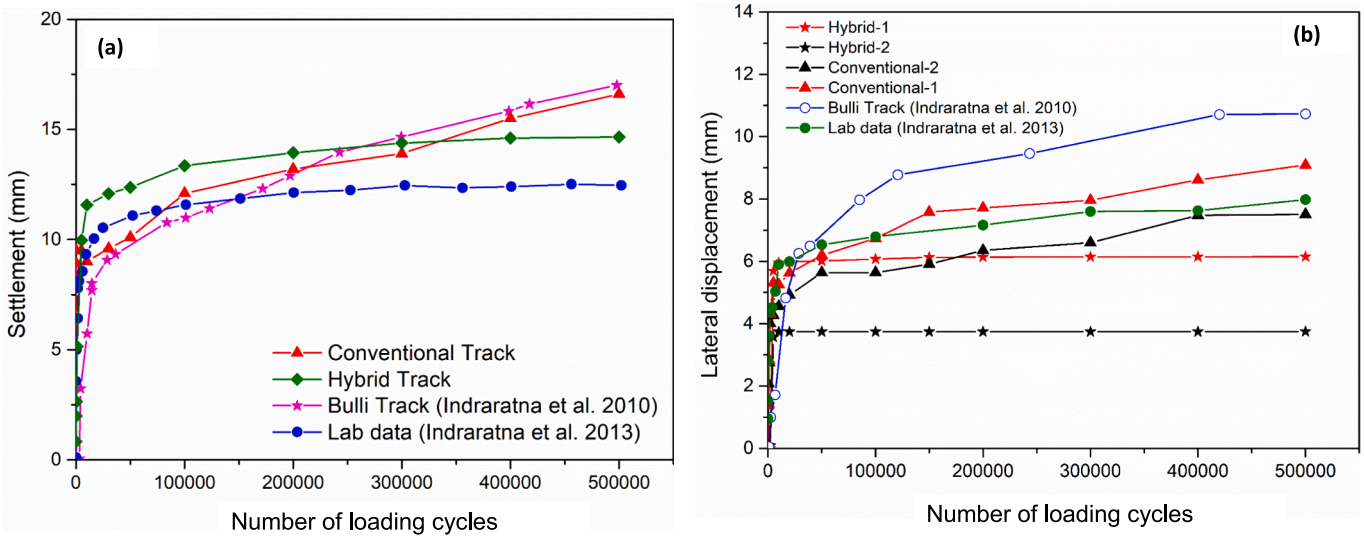

Fig. 17. Measured vertical settlement and lateral displacement of the hybrid track (Data source: *Indraratna et al. 2022*).

The salient findings for this paper can be concluded as below:

- The permanent deformation response of SFS + CW + RC mixtures was investigated based on cyclic triaxial results. These results indicated that under lower cyclic deviatoric stress (16 kPa) the mixtures with $R_b \leq 40\%$ could attain plastic shakedown, but when the deviatoric stress increased to 64 and 112 kPa, only those mixtures with $R_b \leq 10\%$ achieved plastic shakedown, the other tested mixtures reached plastic creep. In light of an empirical model, $R_b \leq 15\%$ was recommended in the mixtures to ensure the material would reach a plastic shakedown under heavy haul trains with a 30-ton axle load.
- The monotonic triaxial tests for RIBS revealed that adding rubber increased the ductility and compressibility of the mixtures, and the peak friction angle decreased when $R_b > 5\%$. Moreover, an increasing amount of rubber in RIBS increased the strain energy density, while the distortional energy decreased, resulting in reduced ballast breakage; in contrast the volumetric strain energy increased as proved by a more compressible behaviour.
- The field trials for RIBS application indicated the beneficial effects of replacing 10 % of traditional ballast with rubber granules within the 150 mm thick lower ballast layer, particularly in reducing vertical stresses (20–30 % reduction) across the depth and alleviating track vibrations (>60 % reduction in acceleration).
- The installation of rubber geogrids under the ballast layer significantly reduced the impact force, ballast deformation, and ballast degradation compared to unreinforced ballast. Among the three different types of rubber geogrids, S2 with a rib thickness of 10.6 mm provided the greatest benefits and behaved better than traditional polymer geogrids. Specifically, the installation of S2 reduced ballast settlement by 31 % and ballast dilation by 21 %, this mitigated ballast breakage by 31 %, and reduced the impact force P_1 and P_2 by 24.5 % and 18 %, respectively.
- The hybrid track's overall accumulated settlement and lateral displacement (reinforced by recycled rubber elements) were smaller than the conventional track. Compared to the standard track, the hybrid track showed a significantly reduced average lateral displacement of about 4 mm while the conventional track (unreinforced) was much higher which was in the range of 8–11 mm when tested by the NTFHR, in the laboratory and in the field. This implies that incorporating rubber elements provided an environmentally friendly solution and a technologically sustainable option for stabilizing tracks, thus leading to an extended life cycle.
- The hybrid track effectively minimized ballast breakage by utilizing the infilled tyre assembly in conjunction with shoulder segments of the tyre catenary, ensuring optimal confining pressure. The reduction of ballast breakage for the hybrid track was $R_{BBI} = 39.2$ % (underneath an actuator), while $R_{BBI} = 42.7$ % for shoulder ballast. This result means that using rubber elements in tracks extended the hybrid track's longevity and decreased the track maintenance costs.

CRediT authorship contribution statement

Yujie Qi: Writing – review & editing, Writing – original draft, Visualization, Validation, Methodology, Investigation, Formal analysis, Data curation, Conceptualization. **Buddhima Indraratna:** Writing – review & editing, Supervision, Resources, Project administration, Funding acquisition, Conceptualization. **Trung Ngo:** Writing – original draft, Validation, Methodology, Formal analysis, Data curation. **Chathuri M.K. Arachchige:** Writing – original draft, Validation, Methodology, Formal analysis, Data curation, Conceptualization. **Suwan Hettiyahandi:** Writing – original draft, Validation, Investigation, Data curation.

Declaration of competing interest

The authors declare that they have no known competing financial interests or personal relationships that could have appeared to influence the work reported in this paper.

Data availability

Data will be made available on request.

Acknowledgements

The authors would like to thank the financial support from the Australian Research Council for ARCLP200200915 and ARCDP220102862. The authors would also like to acknowledge the financial and technical support from industry partners including Sydney Trains, SMEC Australia Pty. Limited, Bentley Systems Pty. Limited, and Bestech Australia Pty. Limited. Some figures were reproduced from the authors' past publications published in Géotechnique, Géotechnique letters, Transportation Geotechnics with kind permissions from ICE and Elsevier.

References

[1] Arachchige CM, Indraratna B, Qi Y, Vinod JS, Rujikiatkamjorn C. Geotechnical characteristics of a rubber intermixed ballast system. Acta Geotech 2021:1–12.
[2] Arachchige CM, Indraratna B, Qi Y, Vinod JS, Rujikiatkamjorn C. Deformation and degradation behaviour of Rubber Intermixed Ballast System under cyclic loading. Eng Geol 2022;307.
[3] ARTC (2010). Earthworks, formation and capping material. ETM-08-1, Australian Rail Track Corporation Limited, Australia.
[4] Arulrajah A, Naeini M, Mohammadinia A, Horpibulsuk S, Leong M. Recovered plastic and demolition waste blends as railway capping materials. Transp Geotech 2020;22:100320.
[5] AS:2758.7 (2015). Standard Australia, Aggregates and rock for engineering purposes Part 7. Railway Ballast. Australia.
[6] ASTM-D7181 (2011). Standard method for consolidated drained triaxial compression test for soils. West Conshohocken, PA, ASTM.
[7] NSWEPA (New South Wales Environment Protection Authority). (2014). "Resource recovery exemption, the protection of the environment operations (waste) regulation 2014—The steel furnace slag exemption." ⟨http://www.epa.nsw.gov.au/resources/waste/rre14-steel-furnace-slag.pdf⟩.
[8] Bathurst RJ, Raymond GP. Geogrid reinforcement of ballasted track. Transp Res Rec 1987;1153:8–14.
[9] Bian X, Jiang J, Jin W, Sun D, Li W, Li X. Cyclic and postcyclic triaxial testing of ballast and subballast. J Mater Civ Eng 2016;28(7):04016032.
[10] Brown S, Kwan J, Thom N. Identifying the key parameters that influence geogrid reinforcement of railway ballast. Geotext Geomembr 2007;25(6):326–35.
[11] Chiaro, G., Indraratna, B., Tasalloti, S. A. and Rujikiatkamjorn, C. (2015). "Optimisation of coal wash–slag blend as a structural fill." *Proceedings of the Institution of Civil Engineers-Ground Improvement* 168(1): 33-44.
[12] DIN (2010). Mechanical vibration—Resilient elements used in railway tracks. Part V: Laboratory test procedures for under-ballast mats. Berlin, German Institute for Standardization. **45673–5**.
[13] Edeskär, T. (2004). Technical and environmental properties of tyre shreds focusing on ground engineering applications, Luleå tekniska universitet.
[14] Fattah MY, Yousif MA, Rasheed ALM. Production of waste rubber-made geogrid reinforcement for strengthening weak soils. Modern applications of geotechnical engineering and construction: Geotechnical engineering and construction. Springer; 2021.
[15] Guo Y, Shi C, Zhao C, Markine V, Jing G. Numerical analysis of train-track-subgrade dynamic performance with crumb rubber in ballast layer. Constr Build Mater 2022;336:127559.
[16] Hennebert P, Lambert S, Fouillen F, Charrasse B. Assessing the environmental impact of shredded tires as embankment fill material. Can Geotech J 2014;51(5):469–78.
[17] Haines D, Wilson W. Strain-energy density function for rubberlike materials. J Mech Phys Solids 1979;27(4):345–60.
[18] Hidalgo Signes C, Martínez Fernández P, Medel Perallón E, Insa Franco R. Characterisation of an unbound granular mixture with waste tyre rubber for subballast layers. Mater Struct 2015;48:3847–61.
[19] Hunt H, Indraratna B, Qi Y. Ductility and energy absorbing behaviour of coal wash–rubber crumb mixtures. International Journal of Rail Transportation 2022:1–21.
[20] Indraratna B, Arachchige CM, Rujikiatkamjorn C, Qi Y, Heitor A. Utilization of granular wastes in transportation infrastructure. Geotech Test J 2024;47(1).
[21] Indraratna B, Ionescu D, Christie H. Shear behavior of railway ballast based on large-scale triaxial tests. J Geotech Geoenviron Eng 1998;124(5):439–49.

[22] Indraratna B, Lackenby J, Christie D. Effect of confining pressure on the degradation of ballast under cyclic loading. Geotechnique 2005;55(4):325–8.
[23] Indraratna B, Mehmood F, Mishra S, Ngo T, Rujikiatkamjorn C. The role of recycled rubber inclusions on increased confinement in track substructure. Transp Geotech 2022;36:100829.
[24] Indraratna B, Ngo NT, Rujikiatkamjorn C. Deformation of coal fouled ballast stabilized with geogrid under cyclic load. J Geotech Geoenviron Eng 2013;139(8):1275–89.
[25] Indraratna B, Ngo T, Ferreira FB, Rujikiatkamjorn C, Shahkolahi A. Laboratory examination of ballast deformation and degradation under impact loads with synthetic inclusions. Transp Geotech 2020;25:100406.
[26] Indraratna B, Ngo T, Ferreira FB, Rujikiatkamjorn C, Tucho A. Large-scale testing facility for heavy haul track. Transp Geotech 2021;28:100517.
[27] Indraratna B, Nimbalkar S, Christie D, Rujikiatkamjorn C, Vinod J. Field assessment of the performance of a ballasted rail track with and without geosynthetics. J Geotech Geoenviron Eng 2010;136(7):907–17.
[28] Indraratna B, Qi Y, Heitor A. Evaluating the properties of mixtures of steel furnace slag, coal wash, and rubber crumbs used as subballast. J Mater Civ Eng 2018;30(1):04017251.
[29] Indraratna B, Qi Y, Jayasuriya C, Rujikiatkamjorn C, Arachchige CM. "Use of recycled rubber inclusions with granular waste for enhanced track performance". Transportation Engineering 2021:100093.
[30] Indraratna B, Qi Y, Malisetty RS, Navaratnarajah SK, Mehmood F, Tawk M. Recycled materials in railroad substructure: an energy perspective. Railway Engineering Science 2022:1–19.
[31] Indraratna B, Qi Y, Ngo TN, Rujikiatkamjorn C, Neville T, Ferreira FB, et al. Use of geogrids and recycled rubber in railroad infrastructure for enhanced performance. Geosciences 2019;9(1):30.
[32] Indraratna B, Qi Y, Tawk M, Heitor A, Rujikiatkamjorn C, Navaratnarajah SK. Advances in ground improvement using waste materials for transportation infrastructure. In: Proceedings of the Institution of Civil Engineers-Ground Improvement; 2020. p. 1–44.
[33] Indraratna B, Rujikiatkamjorn C, Salim W. Advanced rail geotechnology–ballasted track. CRC Press; 2023.
[34] Indraratna B, Sun Q, Grant J. Behaviour of subballast reinforced with used tyre and potential application in rail tracks. Transp Geotech 2017;12:26–36.
[35] Indraratna B, Sun Q, Heitor A, Grant J. Performance of rubber tire-confined capping layer under cyclic loading for railroad conditions. J Mater Civ Eng 2018;30(3):06017021.
[36] Jayasuriya C, Indraratna B, Ngo TN. Experimental study to examine the role of under sleeper pads for improved performance of ballast under cyclic loading. Transp Geotech 2019;19:61–73.
[37] Lackenby J, Indraratna B, McDowell G, Christie D. Effect of confining pressure on ballast degradation and deformation under cyclic triaxial loading. Géotechnique 2007;57(6):527–36.
[38] Le Pen L, Milne D, Thompson D, Powrie W. Evaluating railway track support stiffness from trackside measurements in the absence of wheel load data. Can Geotech J 2016;53(7):1156–66.
[39] Lee J, Salgado R, Bernal A, Lovell C. Shredded tires and rubber-sand as lightweight backfill. J Geotech Geoenviron Eng 1999;125(2):132–41.
[40] Leshchinsky B, Ling HI. Numerical modeling of behavior of railway ballasted structure with geocell confinement. Geotext Geomembr 2013;36:33–43.
[80] Naeini M, Mohammadinia A, Arulrajah A, Horpibulsuk S. Cyclic behavior of semi-rigid recovered plastic blends in railway track substructure. Transp Geotech 2021;28.
[41] Naeini M, Mohammadinia A, Arulrajah A, Horpibulsuk S, Leong M. Stiffness and strength characteristics of demolition waste, glass and plastics in railway capping layers. Soils Found 2019;59(6):2238–53.
[42] Navaratnarajah SK, Indraratna B. Use of rubber mats to improve the deformation and degradation behavior of rail ballast under cyclic loading. J Geotech Geoenviron Eng 2017;143(6):04017015.
[43] Ngo T, Indraratna B, Coop MR, Qi Y. Quasi-static analysis of vertically loaded rock-socketed pile group partially embedded in multilayered saturated rock-soil mass. Géotechnique 2023.
[44] Ngo TN, Indraratna B, Rujikiatkamjorn C. Improved performance of ballasted tracks under impact loading by recycled rubber mats. Transp Geotech 2019;20:100239.
[45] Nuzaimah M, Sapuan S, Nadlene R, Jawaid M. Recycling of waste rubber as fillers: A review. IOP Conference Series: Materials Science and Engineering. IOP Publishing; 2018.
[46] Pirozzolo L, Sol-Sánchez M, Moreno-Navarro F, Martínez-Montes G, Rubio-Gámez M. Evaluation of bituminous sub-ballast manufactured at low temperatures as an alternative for the construction of more sustainable railway structures. Mater Constr 2017;67(327):e128–.
[47] Qi Y, Indraratna B. Energy-based approach to assess the performance of a granular matrix consisting of recycled rubber, steel-furnace slag, and coal wash. J Mater Civ Eng 2020;32(7):04020169.
[48] Qi Y, Indraratna B. The effect of adding rubber crumbs on the cyclic permanent deformation of waste mixtures containing coal wash and steel furnace slag. Géotechnique 2022:1–22.
[49] Qi Y, Indraratna B. Influence of rubber inclusion on the dynamic response of rail track. J Mater Civ Eng 2022;34(2):04021432.
[50] Qi Y, Indraratna B, Heitor A, Vinod JS. Effect of rubber crumbs on the cyclic behavior of steel furnace slag and coal wash mixtures. J Geotech Geoenviron Eng 2018;144(2):04017107.
[51] Qi Y, Indraratna B, Heitor A, Vinod JS. The influence of rubber crumbs on the energy absorbing property of waste mixtures. Geotechnics for Transportation Infrastructure. Springer; 2019. p. 271–81.
[52] Qi, Y., Indraratna, B. and Tawk, M. (2020). Use of Recycled Rubber Elements in Track Stabilisation. Geo-Congress 2020: Geo-Systems, Sustainability, Geoenvironmental Engineering, and Unsaturated Soil Mechanics, American Society of Civil Engineers Reston, VA.
[53] Qiang W, Jing G, Connolly DP, Aela P. The use of recycled rubber in ballasted railway tracks: A review. J Clean Prod 2023;138339.
[54] Ross DE. Use of waste tyres in a circular economy. London, England: SAGE Publications Sage UK; 2020.
[55] Sai Malisetty R, Indraratna B, Qi Y, Rujikiatkamjorn C. Shakedown response of recycled rubber-granular waste mixtures under cyclic loading. Géotechnique 2022:1–21.
[56] Siddiqui A, Indraratna B, Ngo T, Rujikiatkamjorn C. Laboratory assessment of rubber grid-reinforced ballast under impact testing. Géotechnique Letters 2023;13(2):1–11.
[57] Sienkiewicz M, Janik H, Borzędowska-Labuda K, Kucińska-Lipka J. Environmentally friendly polymer-rubber composites obtained from waste tyres: A review. J Clean Prod 2017;147:560–71.
[58] Sol-Sánchez M, Thom N, Moreno-Navarro F, Rubio-Gamez M, Airey G. A study into the use of crumb rubber in railway ballast. Constr Build Mater 2015;75:19–24.
[59] Suiker AS, Selig ET, Frenkel R. Static and cyclic triaxial testing of ballast and subballast. J Geotech Geoenviron Eng 2005;131(6):771–82.
[60] Sun Q, Indraratna B, Ngo NT. Effect of increase in load and frequency on the resilience of railway ballast. Géotechnique 2019;69(9):833–40.
[61] Tawk M, Qi Y, Indraratna B, Rujikiatkamjorn C, Heitor A. Behavior of a mixture of coal wash and rubber crumbs under cyclic loading. J Mater Civ Eng 2021;33(5):04021054.
[62] Duboudin T. Australian rail spend to average $A 14.4bn over next five years. International Rail Journal Categories: Australia/NZ, Financial, Infrastructure, News 2022. https://www.railjournal.com/financial/australian-rail-spend-to-average-a-14-4bn-over-next-five-years/.